Non-contact method used to determine the swelling/shrinking coefficients under CO2 sorption/desorption on an HNBR O-ring - Study of coupling with temperature and pressure

Eric Lainé, J.C. Grandidier, G. Benoit, B. Omnès, Séverine A.E. Boyer

Polymer Testing 85 (2020) 106411

Contents lists available at ScienceDirect

Polymer Testing

journal homepage: http://www.elsevier.com/locate/polytest

Test Method

Non-contact method used to determine the swelling/shrinking coefficients under CO_2 sorption/desorption on an HNBR O-ring - Study of coupling with temperature and pressure

E. Lainé [a,*], J.C. Grandidier [a], G. Benoit [a], B. Omnès [b], S.A.E. Boyer [a]

[a] Institut Pprime, CNRS, ISAE-ENSMA, Université de Poitiers, F-86962, Futuroscope, France
[b] Centre Technique des Industries Mécaniques, F-44308, Nantes Cedex 3, France

ARTICLE INFO

Keywords:
Elastomer seal
Coupling environment
Thermal expansion
CO_2 sorption and desorption
Swelling
HNBR

ABSTRACT

To make use of an O-ring under different pressures and temperatures and to procedure predictive numerical simulations of its use, it becomes important to identify the O-ring behavior under coupled CO_2 sorption (i.e. swelling) and desorption (i.e. shrinking) together with the effect of temperature. Therefore, the presented study deals with an experimental non-contact measurement technique to identify the swelling and shrinking coefficients during pressurization and depressurization under carbone dioxide (CO_2) of an HNBR O-ring. In order to ensure the feasibility of CO_2 sorption (or desorption) measurement from the non-contact method, a purely thermal expansion test permits to identify the thermal expansion coefficient of HNBR, which is well known by other methods including a standard. Numerical simulations complete this section. The simulations ensure that the chosen analysis methodology allows direct identification of swelling and shrinking coefficients and thus determine the seal volume change. CO_2 pressurization and CO_2 depressurization tests at pressures (2, 4 and 6 MPa) under isothermal conditions (60 and 130 °C) and a coupled temperature-pressure CO_2 tests are conducted. The measurements made during these tests show that the CO_2 swelling and shrinking coefficients are independent of pressure but temperature dependent. Besides, a good measurements reproducibility was observed and the order of magnitude of these coefficients leads to a strain in the same order as the thermal strain.

1. Introduction

When polymer components are subjected to a gaseous environment, gas diffusion can significantly affect the behavior of the polymer and modify as well the performance and the functional lifetime of the product, for instance seal. Indeed, the dissolution of the gases inside the material locally causes geometrical deformation due to the deformation of the chemical bonds between the molecular chains. The phenomenon is called plasticization. These effects evolve with temperature and pressure applied by the environment. Sealing rings are prone to the so called plasticization, and must resist to it in order to perform their function throughout their use. Hydrogenated Nitrile Butadiene Rubbers (HNBRs) are used classically in sealing applications (flexible offshore pipes), for oil and gas distribution and consequently this material is in contact with carbon dioxide (CO_2) and methane (CH_4). The mechanical, thermal and chemical resistance properties can be tailored to suit the application by selecting suitable base chemistries [1–3], such as gas diffusion inside the sealing product. However, if some general relationships between composition and performance of elastomers products are reported, a constantly increasing demand remains to get information on how to predict materials behavior in real applications which experience complex mechanical loads in aggressive chemical environments. Despite its importance in sealing, the fundamental understanding of mechanical behavior in elastomeric seals is still incomplete. For example, the coupling between thermal diffusion and swelling is unknown. To improve knowledge of the behavior of elastomers under gaseous environment and during rapid decompression period, further investigation performing new measurements during CO_2 sorption (pressurization) and desorption (depressurization) exposure are required. They are needed to develop fully predictive models describing the combining effects of gases and mechanical loading on elastomeric seals.

First of all, the swelling of polymers is a well-known consequence of fluid sorption [4,5] and this effect is severe with elastomer components

* Corresponding author.
E-mail address: eric.laine@ensma.fr (E. Lainé).

https://doi.org/10.1016/j.polymertesting.2020.106411
Received 20 September 2019; Received in revised form 29 January 2020; Accepted 7 February 2020
Available online 14 February 2020

[6–10]. The volume change phenomenon has been widely discussed in the literature, particularly in the case of carbon dioxide (CO_2) [1,6,9,11–14] and to a lesser extent hydrogen (H_2) [15]. Reported data concern variety of thermoplastics (PEEK, PS, LLDPE, PTFE, PMMA, PET, PP, PVDF, … [12]) in CO_2, but also rubbers and elastomers such as HNBR [1,13,16], NBR [14,16], EPDM [14,16], SBS block [12], PDMS [17,18], FKM [16], PTFE [16], ACM [16], VMQ [16], and rubber polymer [19]. As an illustration, Bonavoglia et al. [11] with the same apparatus described by Rajendran et al. measured by direct visualization the swelling [15]. Four different materials have been tested: PMMA, TFE/PMVE copolymer, PTFE and PVDF with temperature variation from 40 °C to 80 °C and pressure up to 20.7 MPa. A cathetometer with an accuracy of 0.01 cm was used to determine the swelling of a polymer disk housed in a view cell. The view cell is a cylindrical vessel with a volume of 50 cm^3. After pressurization of the cell with CO_2, the change in the diameter of the disk is measured until equilibration. Also, assuming isotropic volume expansion, the percentage of swelling was then calculated. Despite a relatively low percentage of expansion of 15–20%, the highest swelling was noticed at the highest temperature. Recently, Schrittesser et al. [13] had used an autoclave equipped with a camera system to measure the impact of several influencing parameters (temperature, saturation pressure, depressurization rate) on the volume change of an HNBR1 (ISO 6072 Standard) (with acrylonitrile content of 36% and a hardness of 86 Shore A) during the pressurization and depressurization phases. The observed volume changes were correlated with the classification of materials according to the NORSOK test standard (2001). However, they were unable to establish a link between the volume changes and the observed rapid gas decompression performance. Indeed, the authors had observed a strong influence on the volume changes and kinetics of the volume changes during decompression, the NORSOK standard ranking does not change.

On the other hand, CO_2 solubility in polymers has often been determined by measuring gas sorption [20] by means of gravimetry [11,21,22] and by spectroscopic methods [23]. Gas solubility has also been quantified by direct observation of polymer swelling [22,24,25]. For instance, Ender [26] developed a linear variable differential transformer (LVDT) method to measure O-ring swelling. Author used this LVDT method on FKM and nitrile rubber O-rings. On depressurization, a post-plasticization "inflation'' effect was caused by internal gas expansion being more rapid than gas out-diffusion. "Sponginess or fracture'' was observed if inflation exceeded "a few percent''. Shenoy et al. [12] also used a LVDT to evaluate CO_2-polymer plasticization of polystyrene-block-polybutadiene-block-polystyrene (SBS) elastomer. At 22 °C under CO_2 pressure, SBS undergoes compression due to hydrostatic pressure. However, sample expansion occurs upon depressurization. At 45 °C, SBS undergoes swelling of 0.7% due to the CO_2 plasticization, while no post-pressurization expansion is observed. The contrasting results are explained by changes in polystyrene (PS) domain molecular mobility and discontinuity in the density-pressure relationship.

However, the realization of in situ measurements on structures, under very high pressure, presents multiple technical difficulties, notably if the sensors are installed inside the chamber. Measurements are often obtained on very small samples or specific specimens whose characteristic volumes are far from industrial seals. Besides, pressure variations of gas generate temperature changes. Thermal diffusion coupling can be expressed during the transient phases of pressure rise and gas diffusion. If the material is out of balance these paths generate complex histories of specific volume changes. Boyer et al. [27] have discriminated, in live from thermodynamical analysis, the volume deformation due to gas solubility in sorption and in desorption modes to the volume deformation due to temperature on PVF_2 (polyvinylidene fluoride) under carbon dioxide pressure constraints. Additionally, the extraction of diffuso-mechanical properties means that the representative coefficients must be tracked in coupling conditions. Mostly thermal, mechanical and gas diffusion effects occur simultaneously. This is commonly observable in elastomer polymers but not only [27,28]. For instance, in previous works, Grandidier et al. [28] have identified key thermo-diffuso-mechanical couplings to characterize the irreversible "explosive decompression failure" (XDF) with the prediction of the diffusion kinetics and of the volume deformations (swelling) of PVF_2 in interactions with CO_2.

Nevertheless, it is still difficult to identify useful diffuso-mechanical properties from the O-rings. The first difficulties are the geometry of the sample. Definitely, the seals geometries are not well suited to conventional mechanical testing. Additionaly, if many works exist in the literature, they generally concern materials made from blocks or plates. There is always the inherent question of the properties of seals that are developed with an industrial process that may differ slightly from those of laboratories. Even if the processes are identical, the curing parameters can change and impact the state of the material. Consequently, the first experimental challenge identified in this paper is to measure the thermal expansion and CO_2 swelling coefficients directly on industrial O-rings. This framework avoids questions about the microstructure of samples compared to samples generated by the industrial process. The second challenge is to perform in situ measurements under different CO_2 gas pressures and different temperatures using a non-contact measurement technique.

The results presented in this article are based on an experimental technique, revisited to be adapted to seals geometries, under extreme conditions so that it can be applied as widely as possible [29–31]. The system has the capability to control the pressure and temperature drop in a chamber with a relatively small volume. In section 2, the material and the mechanical behavior model are introduced, also the test to measure the coefficient of thermal expansion of rubber. In section 3, the test bench and the experimental in situ measurement technique are described respectively as well as the numerical tool to evaluate experimental measurements. In section 4, the results and the discussions about the values of CO_2 swelling and shrinking coefficients in isothermal conditions (60 and 130 °C) and coupled temperature-pressure CO_2 (2, 4, 6 MPa) test are reported. The conclusions of this work are reported in Section 5.

2. Material

2.1. Material and sample

One elastomer type, a hydrogenated nitrile rubber (HNBR) was selected for these investigations [29]. The hardness of the vulcanized compounds is 80 Shore A. The recipicies of rubber are compounded as described in Table 1. The matrix polymer is 96% saturated with 36% acrylonitrile content. HNBR was vulcanized with peroxide curing systems and the quantity of reinforced fillers (Carbon Black) is fixed at 70 phr. HNBR selected can be used to 150 °C without thermal damages.

The nominal dimensional characteristics of the O-rings are 50.17 × 5.33 mm, respectively the inner diameter and the cross-section diameter.

2.2. Constitutive law

To describe the mechanical behavior of the elastomer, the neo-

Table 1
Composition of the HNBR assessed in the paper.

Material	HNBR phr[a]
HNBR	100
N-330 HAF carbon black	70
Antioxydant agent	1.5
Vulcanizing agent	8
Vulcanizing accelerator	2

[a] Parts per hundred rubber parts in weight.

Hookean compressible form of the strain energy density function W was chosen. This model allows describing the moderate strains as part of this study [32–34]. The Neo-Hookean model is typically formed of the deviatoric and the volumetric terms. Following compression tests on O-rings at different temperatures and CO_2 pressures, the authors [29] showed that the material parameters were a function of temperature and CO_2 pressure. Consequently, the Neo-Hookean model is extended as follows:

$$W = C_{10}[P_{CO2}, T](\overline{I_1} - 3) + D_1[P_{CO2}, T](J^{el} - 1)^2 \quad (1)$$

where C_{10} and D_1 are material parameters dependent on temperature and CO_2 pressure [29]. $\bar{I}_1$is the first deviatoric strain invariant defined as:

$$\overline{I_1} = \overline{\lambda_1}^2 + \overline{\lambda_2}^2 + \overline{\lambda_3}^2 \quad (2)$$

where $\lambda i;$ is the deviatoric principal stretches ($\lambda i; = J^{-1/3}\,\lambda_i$) and λ_i are the principal stretches. The scalar J^{el} is the elastic volume ratio defined as:

$$J^{el} = J/J^{th} \quad (3)$$

where J is the total volume ratio and J^{th} is the thermal volume ratio as:

$$J^{th} = (1 - \varepsilon_{th})^3 \quad (4)$$

where ε_{th} is the thermal expansion strain given in differential form:

$$d\varepsilon_{th} = \alpha_{th} dT \quad (5)$$

with α_{th} the isotropic thermal expansion coefficient. To convert to the total thermal expansion form required by Abaqus©, this relationship (5) must be integrated from a suitably chosen reference temperature, T_0.

If the thermal expansion coefficient is constant, then equation (5) is written as follows:

$$\varepsilon_{th} = \alpha_{th}(T - T_0). \quad (6)$$

This hypothesis is maintained throughout this work although one could consider that this coefficient is dependent on temperature. Thanks to the last equation, the thermal strain in the stabilized part is only calculated. The transient phase cannot be represented correctly, as the temperature diffusion is not taken into account because of the gradients. The analytical solution obtained above will then allow comparison with the experimental responses.

However, as the results of this study will display, the CO_2 swelling (or shrinking) coefficient (α_{CO_2}) is temperature dependent. Since only two temperatures were studied, this dependence will be considered linear.

Thus, if the CO_2 swelling (or shrinking) coefficient (α_{CO_2}) is constant, then equation (6) is written as follows:

$$\varepsilon_{pressure\_CO_2} = \alpha_{CO_2}(P - P_o) \quad (7)$$

where $\varepsilon_{pressure\_CO_2}$ is the strain due to CO_2 pressure that is referred to in this work as "pressure strain". If the coefficient of CO_2 pressure is a linear function of temperature, then it is written as follows:

$$\alpha_{CO_2}(T) = a_{CO_2} T + b_{CO_2}. \quad (8)$$

The "pressure strain" in differential form is written:

$$d\varepsilon_{pressure\_CO_2} = (a_{CO_2} T + b_{CO_2}) dP_{CO_2} \quad (9)$$

with the temperature T and the pressure P which are a function of time $f(t)$ and $g(t)$ respectively. To convert to the "total pressure strain" form, this relationship must be integrated from a suitably chosen reference time:

$$\int_{t_0}^{t} d\varepsilon_{pressure\_CO_2} = \int_{t_0}^{t} (a_{CO_2} f(t) + b_{CO_2}) \frac{dg(t)}{dt} dt. \quad (10)$$

If it is considered that the temperature and the CO_2 pressure varie linearly over time between two measuring points, then the function $f(t)$ is written:

$$f(t) = \frac{(T_{i+1} - T_i)}{t_{i+1} - t_i} t + \frac{(T_i t_{i+1} - T_{i+1} t_i)}{t_{i+1} - t_i} = a_T t + b_T \quad (11)$$

and the function $g(t)$ passing through zero is written:

$$g(t) = \frac{(T_{i+1} - T_i)}{t_{i+1} - t_i} t = a_P t. \quad (12)$$

So equation (10) becomes:

$$\varepsilon_{pressure\_CO_2} = \sum_{0}^{n} \int_{t_i}^{t_{i+1}} [a_{CO_2}(a_T T + b_T) + b_{CO_2}] a_p dt. \quad (13)$$

The integration of equation (13) gives:

$$\varepsilon_{pressure_{CO_2}} = \sum_{i=1}^{n} \frac{a_{CO_2} a_P a_T}{2} \left(t_{i+1}^2 - t_i^2\right) + a_P(a_{CO_2} b_T + b_{CO_2})(t_{i+1} - t_i). \quad (14)$$

$$\varepsilon_{pressure\_CO_2} = \sum_{i=1}^{n} \Delta\varepsilon_{presure\_CO_{2i}} \quad (15)$$

2.3. Reference measurement of the thermal expansion under air of the material according to the standard

Initially, thermal expansion tests were carried out, according to the conditions of the ISO 11359-2 standard [35], on small parallelepipedic samples of 5 mm × 5 mm section and 10 mm height. Expansion measurements are obtained by applying a thermal profile to the specimens three times and following the expansion or contraction as a function of temperature. Three cycles are applied with temperature rise or fall speeds of 5 °C/min with 5-min stabilization steps. Table 2 gives the thermal expansion coefficients measured at different temperatures for the three HNBR samples.

2.4. Reference measurement of thermal expansion under nitrogen (DMA) at O-ring

A second method, which is a non-standardised approach, can also identify an average coefficient of thermal expansion over a given temperature range. This consists of a DMA (Dynamic Mechanical Analyser) test in compression, placing a piece of O-ring between two platters: a fixed and a mobile one. The displacement of the moving plate, regulated to a force of 0.001 N to ensure contact with the O-ring, is measured

Table 2
Thermal expansion coefficients $\propto_L]_{T_0}^{T}$ $10^{-6}(C^{-1})$ according to ISO 11359-2 standard and to compression DMA.

Temperature (°C)	ISO 11359-2 standard				Compression DMA			
	Sample			Mean value	Sample			Mean value
	1	2	3		1	2	3	
23	/	/	/	/	/	/	/	/
40	177	152	156	162	146	156	149	150
50					154	165	160	160
60	180	159	159	166	165	175	165	168
70					172	179	168	173
80	183	168	163	171	175	181	170	175
90					176	181	170	176
100	183	174	164	174	177	180	171	176
110					176	179	171	175
120	183	176	165	175	177	177	172	175
130					177	178	172	176

during the application of a temperature ramp. The thermal history is a heating from 23 °C to 130 °C at a speed of 5 °C/min with 5-min stabilization steps. These conditions were chosen to be similar to those of ISO 11359-2 standard [35]. From this measurement, the relative stretching $\Delta L/L_0$ (with ΔL the elongation and L_0 the initial height which corresponds to the diameter of the torus), corresponds to the thermal strain. At each step $\Delta L/L_0$ is plotted as a function of temperature, and according to equation (6) the thermal expansion coefficient can be determined as a function of the temperature.

Three tests were carried out directly on three different O-rings, each 10 mm long. Table 2 gives the thermal expansion coefficients measured at different temperatures for the three HNBR samples. In this temperature range, both protocols (ISO 11359-2 standard and compression DMA) provide values very close to the thermal expansion coefficient of an industrial O-ring.

3. Experimental

3.1. Experimental device

An Instron 8802 servohydraulic fatigue machine (Fig. 1) was fitted with a pressure and temperature regulated chamber which allows mechanical testing in gaseous nitrogen, hydrogen or carbon dioxide up to 40 MPa and 150 °C. For safety reasons related to hydrogen, the volume of the chamber is rather small (1.77 L with a diameter of 150 mm and length of 100 mm). The device is named HYCOMAT. More information on this device can be found in previous papers [29,36–38]. To observe the specimen, the vessel has a front and a back optical access through a central cylindrical sapphire window of 40 mm diameter.

The dynamometer, with a maximum capacity of 20 kN, can operate up to a frequency of 20 Hz. Its maximum stroke is 25 mm (limitation to the dimensions of the lower water jacket). However, the height of the chamber limits the dimensions of the various assemblies and test pieces. The traction machine is provided with an external load cell and a pressurized column containing a pressure compensated internal load cell. To avoid the force due to the reaction of sealing, a direct measurement is performed with an internal load cell.

For the expansion test (thermal and gas), the O-ring is placed on a rigid U-shaped structure positioned horizontally as shown in Fig. 1b and c. This support is connected to the fixed jaw of the machine. Simply placed on the board, they are free to expand in all three directions. Beforehand, the lower plate is lubricated to improve the sliding between the latter and the O-ring. Since the objective is to identify the coupling parameters, it is easier to measure this phenomenon in a free configuration. If the O-ring was clamped in its groove, then the coupling would generate a stress inside the groove. Thus, measuring the strain inside the groove would be very difficult.

The pressurization under CO_2 of the chamber consists in injecting CO_2 into it initially filled with air at atmospheric pressure. Three pressures are imposed 2, 4 and 6 MPa and two temperatures are selected (60 and 130 °C). Thus, the actual pressure (partial pressure) in CO_2 can be calculated by considering the amount of CO_2 contained in the air with that added to reach the set pressure (2, 4 or 6 MPa). In Table 3, the corresponding CO_2 partial pressure is given for each desired pressure. In the rest of the document, to simplify reading, only the desired pressures are indicated.

The CO_2 pressure and temperature values comply with both NACE [39] and NORSOK M710 [40] standards, and under NACE conditions the pressure is set at 5.2 MPa at room temperature. To study the impact of temperature and pressure on the diffusion effect (NORSOK M710), the values were gradually increased to 130 °C and 6 MPa. The temperature limit was imposed by the thermal resistance of the HNBR.

In addition, it should be noted that during these tests, the decompression rate is imposed by the machine [29]. It is not possible to control the decompression rate.

3.2. Technique of dilatation measurement on seals

An in situ strain measurement technique is applied. It is based on the follow-up of small markers drawn on the seal. The displacement of the markers is recorded in situ into the thermo-regulated gas chamber. To validate this technique:

Table 3
Equivalent imposed pressure - partial pressure of CO_2.

Imposed pressure of CO_2 (MPa)	2	4	6
Partial pressure of CO_2 (real) (MPa)	1.899	3.899	5.899

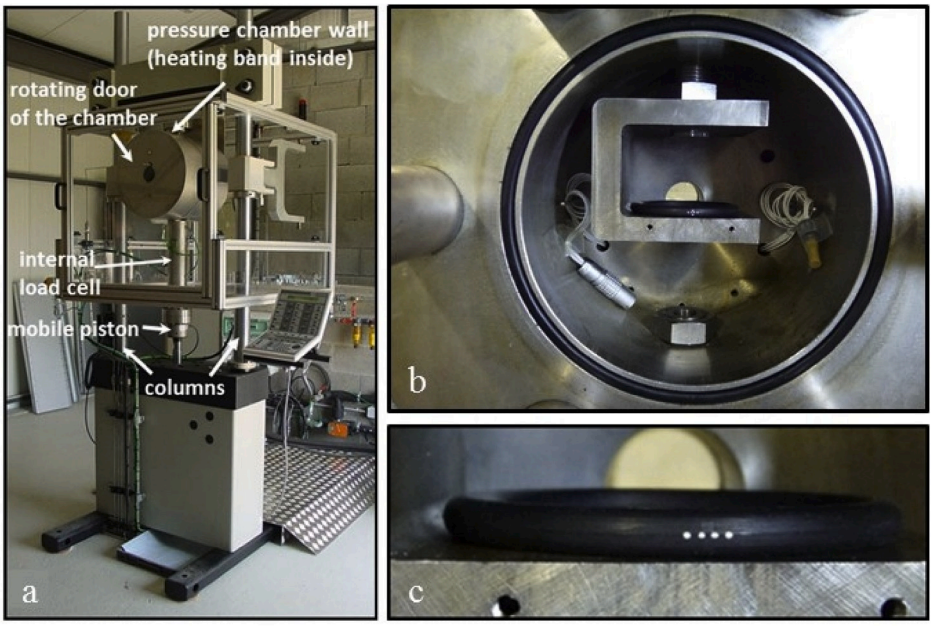

Fig. 1. (a) Global view of HYCOMAT and (b) Magnification of the pressure CO_2 chamber of the test fixture. (c) Positioning the O-ring in the chamber [29].

- An evaluation of the sensibility of positions of markers and a quantification of the defects was performed with FEA (Finite Elements Analysis, see part 3.2.2.) approaches;
- With industrial O-rings, the thermal expansion under air is characterized and compared with measurements obtained with standards.

3.2.1. Non-contact extensometry (markers tracking method)

From the point of view of metrology, a system of non-contact extensometry is used [29,38]. This method of markers, developed within the laboratory, has the advantage of being usable in extreme conditions (very high temperatures, high pressures). Fig. 2 illustrates a local view of a seal with markers (2 or 4) placed on the generatrix of the O-ring. This generatrix corresponds to the parting line of the O-ring, it is represented by a dotted line. The classical technique consists in following the displacements of the barycentres of the markers in the plane of a couple of them. From this measurement of the relative displacement between two markers, a "local deformation" is deduced which is called deviation **(dev)**.

$$\text{dev}\ (\%) = \frac{\Delta L}{L_0} = \left(\frac{\sqrt{\left(X_k^i - X_k^j\right)^2 + \left(Y_k^i - Y_k^j\right)^2} - \sqrt{\left(X_0^i - X_0^j\right)^2 + \left(Y_0^i - Y_0^j\right)^2}}{\sqrt{\left(X_0^i - X_0^j\right)^2 + \left(Y_0^i - Y_0^j\right)^2}} \right) \times 100 \tag{16}$$

where, ΔL is the change of length and L_0 is the initial length between two markers.

If the thermal strain is calculated by equation (6), then the thermal expansion coefficient can be directly deduced by the following relationship:

$$\alpha_{th} = \text{dev} / (T - T_0). \tag{17}$$

In a similar manner if the "pressure strain" is calculated by equation (7), then the CO_2 swelling (or shrinking) coefficient can be directly deduced from the deviation, for each configuration. Thus, from equation (16) it is possible to replace the temperature variable and to write:

$$\alpha_{CO_2} = \text{dev} / (P - P_0). \tag{18}$$

Swelling and shrinking coefficients under CO_2 are identified in the same way as the thermal expansion coefficient. Thus from the optical measurement, and by tracing the ratio of the change of length (ΔL) by the initial considered length (L_0), as a function of the CO_2 pressure, the swelling or shrinking coefficient under CO_2 can be obtained directly, respectively according to equation (18).

More precisely, to perform measurements during the experimental test, four markers are drawn on the O-ring. Consequently, this marking allows having a horizontal measurement of the dimensional changes by taking them two by two. The camera is centered between markers 2 and 3 (Fig. 2). Markers 1 and 4 are the furthest away. Horizontal deviations along the generatrix at the parting line are measured respectively between markers 1 and 4; and markers 2 and 3. These horizontal deviations are noted DevH14 and DevH23 respectively in the following part of the paper. The measurement of deviations between the nearest (2 and 3) and furthest (1 and 4) markers respectively, allows the values to be framed and the quality of the measurements to be assessed with these markers. Notice that the tests have been carried out with vertical markers, but they do not allow a clear measurement to be obtained without taking into account the evolution of the focal point (because of O-ring shape). Moreover, the knowledge of the distances from the object to the camera must be measured accurately, which is not easy in the environment of the pressure machine. Concerning to this experimental technique, a direct link can be expected between marker alignment errors and errors in the measurement of O-ring expansion. To quantify the effects of such a misalignment error, a numerical simulation is performed in the following paragraph.

The volume of an O-ring is calculated using the following formula:

$$V^{O-ring} = 2\pi^2 r^2 R \tag{19}$$

where r is the radius of the cross-section and R is the median radius (average of inner and outer radii). For the studied O-ring (50.17 mm × 5.33 mm), r and R have as values respectively 2.665 mm and 27.75 mm. A volume change of the O-ring results in an increase (or decrease) in radii, such that according to a thermal condition, for example, the radius of the section changes from r to $r+\Delta r$ and the median radius changes from R to $R+\Delta R$. Δr and ΔR are respectively the variation of the cross-section radius and the variation of the median radius subjected to a thermal difference. Then under the assumption of isotropic volume expansion, variations are written:

$$\Delta r = \text{dev} \times r \text{ and } \Delta R = \text{dev} \times R \tag{20}$$

Therefore, the change in volume (swelling-*Sw*) due to thermal or CO_2 pressure is calculated as follows:

$$Sw = \frac{V^{O-ring} - V_0^{O-ring}}{V_0^{O-ring}} = (1 + \text{dev})^3 - 1. \tag{21}$$

3.2.2. Numerical validation of the measurement protocol for expansion of the O-ring

Numerical simulations of expansion of the seal are implemented to confirm the ability of the proposed analytical methodology (deviation measurement) to identify an expansion coefficient. The effect of a marker positioning error is explored. These simulations are performed using the commercial FEA (Finite Elements Analysis) software ABAQUS© [32]. A quarter of the O-ring is designed and the material symmetries are used to fit the whole O-ring. The two compression plates are

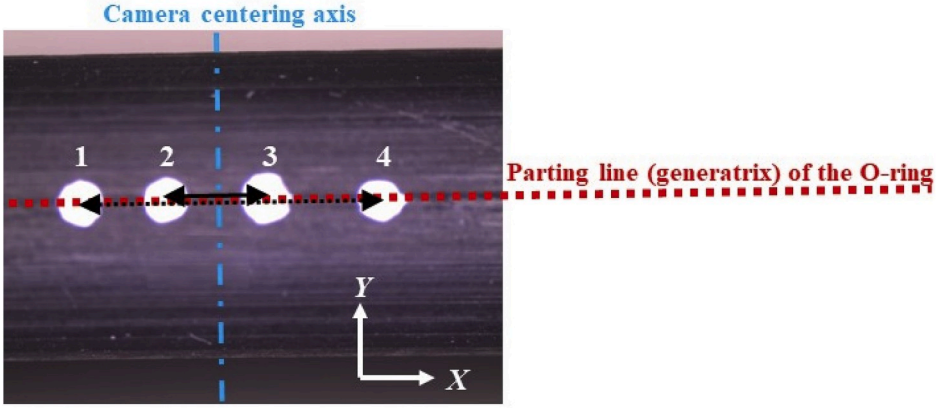

Fig. 2. Measurement horizontal deviations (devH14 & devH23) - complex markers Tracking Method [29].

represented by discrete rigid surfaces. The contact is managed between the different parts (seal, lower and upper plates) with a friction coefficient of $\mu = 0.2$ to ensure the stability of the numerical simulation. A parametric study of the friction coefficient showed that the compression response was independent of the friction coefficient in the observed deformation range. The seal is meshed with 43120 hexahedral elements (185501 nodes) with linear interpolation and hybrid formulation (C3D20H in Abaqus®). The material parameters of the behavior law for HNBR are those given by the authors [29] and the expansion coefficient is fixed at 170 10^{-6} °C^{-1}. The numerical simulation consists in reproducing the thermal expansion of the O-ring during a thermal ramp from 20 °C to 130 °C imposed on the entire range. The field of thermal strains is homogeneous with a local value of 0.680% of thermal strain at 60 °C.

From the experimental point of view, the strain (deviation) is calculated from the displacements of the barycentre of the markers (see part 3.2.1.). In the numerical simulation, the horizontal deviations are computed from the displacements of the mesh nodes that correspond to the position of the marker barycentres. Fig. 3 shows the superposition of the mesh defined in the numerical simulation and the image of the seal with the four markers in the initial state. The numerical deviations are calculated by considering two markers perfectly positioned on the gasket generator (2–3 and 1–4) and two "badly positioned" markers (2′-3′ and 1′-4′). This test permits to quantify the influence of the radius of greatest curvature on the measurement of the deviation and a positioning error.

By comparing these numerical deviations (2–3, 1–4, 2′-3′ and 1′-4′) calculated by equation (16), it appears that the deviation measurement variation is less than 10^{-4}. A measurement of the horizontal deviation does not present any major difficulty because the two markers remain in almost the same plane throughout the swelling. Besides, the numerical simulation results show that the distance between horizontal tasks or positioning errors does not influence the result. The measurement of the horizontal deviation (DevH) is therefore validated to quantify the expansion in a pressurized environment. This demonstration is only valid in the case of a perfectly thermally isotropic material and a seal similar to the one used in the numerical simulation.

3.2.3. Validation of in situ O-ring measurement technique

The non-contact measurement method is not easy to set up (lighting, camera resolution) in a technical environment (small and desaxed speaker glass), and the observed surface of the seal is not a flat surface, the reliability and robustness of this measurement should be prove. The technique is evaluated on thermal expansion measurements in such a technical environment.

Four tests (number 1 to 4) were realized and the pressure corresponds at ambient condition. For two tests, a jump of temperature is applied between 20 and 60 °C for both other tests the temperature evolves, 60 and 130 °C. Table 4 presents the results where measured horizontal deviations and thermal expansion coefficients are calculated according to equations (16), (17), the average value of the thermal expansion coefficient determined for each condition (temperature, pressure). Finally, the volume change is given according to equation (21).

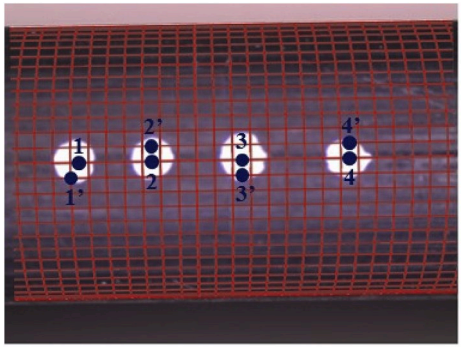

Fig. 3. Measures deviations from node displacements (seal).

The temperature transitions (20–60 °C, 60–130 °C) generated by the system take 2 h, the expansion measurements evolve synchronously as shown in Fig. 4. The measurement and test system appears reproducible.

Test 5 describes a thermal test by successif jump. After about 10 h at 60 °C (rise and plateau) the seal undergoes a new ramp from 60 °C to 130 °C and then a hold time of more than 7 h at this last temperature. The stabilization of strains has been obtained for each case. Fig. 5a shows the temperature curve and measurements of the two deviations for Test 5. The reproducibility is confirmed, transient phase is always present. The temperature curve shows an overshoot of a few degrees after the 20–60 °C and 60–130 °C ramps. This exceeding the temperature set point for about 1 h has almost no impact on the response. According to equation (6), the analytical response in the stabilized phase gives at 60 and 130 °C, with the data identified in Table 6, the red curves in Fig. 5a. A good prediction is found with the values of the thermal expansion coefficients identified at 60 and 130 °C. Besides, there is no thermal effect on the material because the thermal history at 60 °C has no impact on the thermal response at 130 °C.

In summarize the reliability and robustness of this measurement can still be seen on these results. Thus, it has been shown that with this technique, it is possible to measure the thermal expansion coefficient on an O-ring. Moreover, the measured values are close to those obtained by more traditional methods: on plate according to the standard (ISO 11359–2) (see part 2.3) and to the DMA (see part 2.4) (Fig. 5b).

Consequently, with this approach, it seems to be possible to identify the sorption and shrinking coefficients and the swelling of the O-ring due to CO_2 pressure (or depressure), provided that it is at least of the same order of magnitude. Conditions combining pressure and temperature changes can also be considered to study couplings between thermal and gas-take expansion.

4. Results and discussions

4.1. In situ characterization of dilations generated by the dissolution of CO_2

4.1.1. CO_2 sorption (pressurization) tests under isothermal

During the CO_2 characterization protocol of the HNBR seal, CO_2 pressurization tests are performed. Fig. 6 shows the measurements of horizontal deviations as a function of the square root of time during CO_2 pressurization at 60 and 130 °C. The transient curves, i.e. before stabilization, have characteristic times identical to the diffusion and therefore give the same response. The measurement errors on deviations are in the range of 2–5% depending on the pressure applied. However, it should be noted that the measurements are quite accurate as they perceive temperature fluctuations during the test in the response. These fluctuations are due to the regulation of the thermal system.

For both temperatures, an increase in the deviation is observed with pressurization under CO_2, reflecting the solubility phase. Fig. 6a (60 °C) shows for the HNBR O-ring that the pressure stabilization time decreases with increasing pressure. Thus, if it takes almost 16 h for a pressure of 2 MPa, it takes just 9 h to 6 MPa. At 130 °C (Fig. 6b), 2 h is the minimum time that allows the stabilization of the seal under pressure at 2, 4 and 6 MPa.

Table 5 shows the deviations obtained for all the tests performed under different temperatures and pressures conditions. For each of the test conditions (temperature and pressure), the deviations are determined by averaging the measurement points beyond the stabilization time after CO_2 absorption from the O-ring. The CO_2 swelling coefficients are calculated from equation (18) for each test condition (initial temperature and pressure). At 60 °C, the deviations for 2, 4 and 6 MPa are respectively 1, 2 and 3%. On the other hand, at 130 °C they are about 40% lower than at 60 °C. For both temperatures (Fig. 6), the CO_2

Table 4
Deviations, Coefficient of thermal expansion and swelling for two temperatures (60 and 130 °C) for different combinations of markers.

Test	Temperature (°C)		Deviation (%)		*Thermal expansion coefficient* $\alpha_L]_{T_0}^{T}$ $10^{-6}(C^{-1})$		Swelling
	Initial	Final	DevH14	DevH23	*Calculus*	*Mean Value*	*Sw (%)*
1	18.50	59.36	0.746	0.698	171–183	165	1.97
2	21.11	59.40	0.560	0.615	146–161		
3	62.03	130.04	/[a]	1.240	182	176	3.67
4	60.08	129.73	1.146	1.258	165–181		

[a] Value not retained.

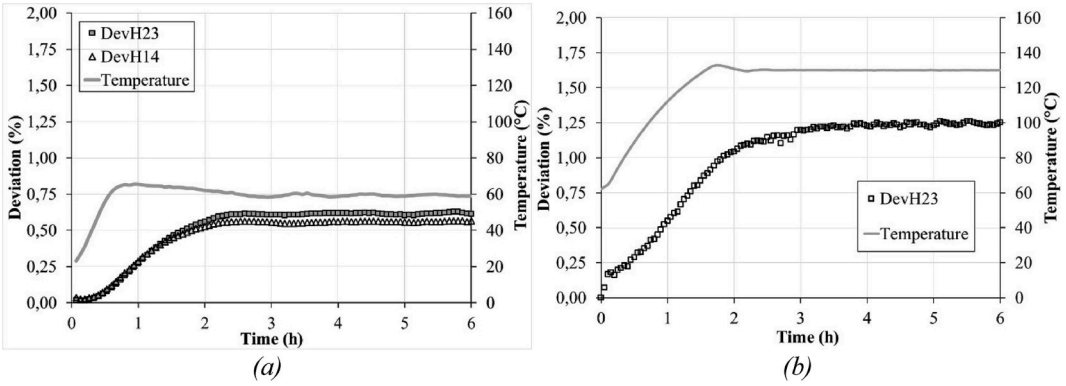

Fig. 4. Thermal expansion test - Evolution of Horizontal deviations and temperature as a function of time (a) test 2 at 60 °C – (b) test 3 at 130 °C.

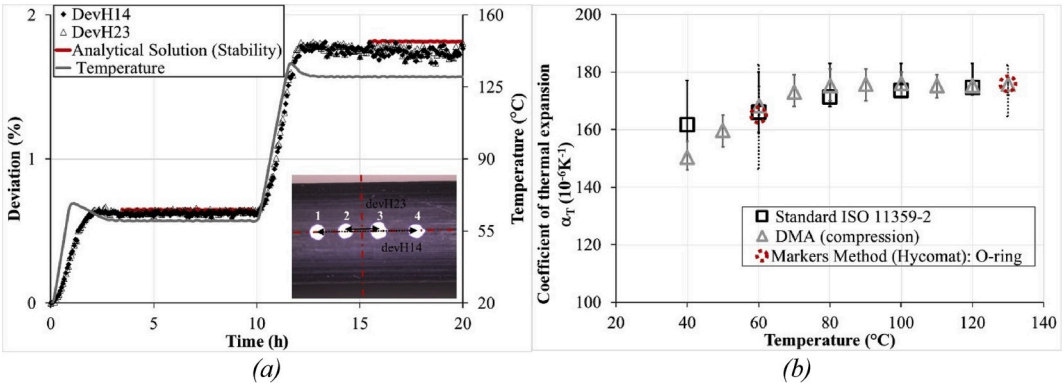

Fig. 5. (a) Thermal ramp test (Test 5) - Evolution of Horizontal deviations and temperature as a function of time – (b) Coefficient of thermal expansion vs. Temperature obtained by different measurement techniques.

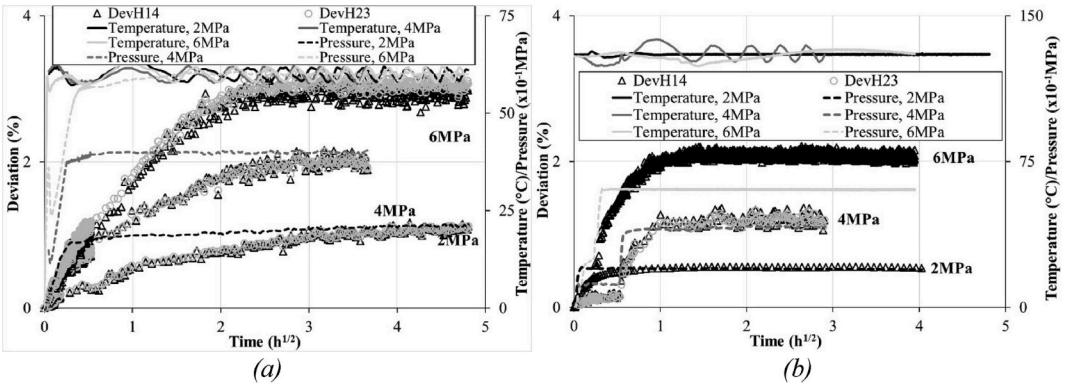

Fig. 6. Pressurization test at different CO_2 saturation pressures at (a) 60 °C – (b) 130 °C.

swelling coefficients are a priori independent of the pressure. The average values at 60 and 130 °C are 5.00 10^{-3} MPa^{-1} and 3.10 10^{-3} MPa^{-1} respectively.

4.1.2. CO_2 desorption (depressurization) tests under isothermal

In the characterization protocol, CO_2 desorption tests are always performed to evaluate irreversible effects generated by diffusion of gas inside the rubber. They are carried to check whether or not the behavior of the HNBR seal has been modified by the absorption of CO_2 at a given pressure. For each temperature, the deviations are measured throughout the CO_2 depressurization until they return to the air and stabilize. Fig. 7 plot the deviation responses at 60 and 130 °C. The three initial saturation pressures that are imposed are approximately 2, 4 and 6 MPa. Note that for the test at 6 MPa and 130 °C, the decompression rate is lower (about a ratio of 2) than for the other tests. In Table 6 are given the values of the deviations measured after stabilization, the CO_2 shrinking coefficients calculated from equation (18) for each test condition (initial temperature and pressure). For both temperatures, the CO_2 shrinking coefficients are at the first order, independent of the pressure. The average values at 60 and 130 °C are 4.70 10^{-3} MPa^{-1} and 3.14 10^{-3} MPa^{-1} respectively in the stabilization phase.

In Table 7, for each initial condition, the pressure for temperature is minimal. Besides, the value of time of maximum swelling in the transient phase and its deviation are also indicated. It can be noticed that, from the early moments, the pressure decreases, the temperature in the autoclave decreases at a rate proportional to the CO_2 pressure. Thus for pressures 2, 4 and 6 MPa and at 60 °C, the temperature decreases by 10, 12 and 13 °C (Table 7) respectively before rising to stabilize at the temperature of the device. At 130 °C, the temperature decreases lower. For example, for the initial CO_2 pressure of 6 MPa, the temperature of the autoclave decreases to 48 °C before rising again. During this stage, the O-ring shrinks (negative deviation), then expands, due to the combined effect of temperature increase and CO_2 pressure decrease (and thus the beginning of desorption). Fig. 7a shows residual deviations (at zero CO_2 pressure) and the maximum deviation which reaches almost 7.69% for the highest conditions (60 °C and 6 MPa) after 20 min and depressurization which corresponds to a 24.58% swelling according to equation (21). After 2h45 the seal returns to its initial position. After more than 22 h, the deviation stabilizes. The stabilization time for a 2 and 4 MPa depressurization is 16 and 20 h respectively. At 130 °C, during the 6 MPa depressurization, the maximum deviation is 0.70%, which corresponds to a 2.21% swelling according to equation (21).

At 130 °C (Fig. 7b), the phenomenon, mentioned above at 60 °C and 6 MPa, is reduced. Thus, if the seal shrinks by about 1% at 60 and 130 °C when the CO_2 pressure decreases, the subsequent swelling is different. It is only 0.70% at 130 °C compared to nearly 8% at 60 °C. It therefore appears that the HNBR seal is more sensitive to CO_2 pressure at 60 °C than at 130 °C because the deviations are greater, resulting in higher deformations. The stabilization times at 60 and 130 °C are proportional to the initial CO_2 pressure. Consequently, when the pressure of carbon dioxide increases then the period of stabilization rises.

4.1.3. Discussion

Fig. 8 graphically presents the deviation measurements occurred during the isothermal tests, these are identified by squares dots for 60 °C and by circles for 130 °C. Consequently, the evolutions respectively during sorption and desorption under CO_2 as a function of the pressure difference of CO_2 (a ΔP_{CO2}) is compared. The evolution could be described by a linear regression with a very high level of concordance.

Fig. 8a displays that after CO_2 sorption, the CO_2 swelling coefficients at 60 and 130 °C are respectively 5.00 and 3.10 10^{-3} MPa^{-1} (slope of linear curve fitting). Fig. 8b shows that after depressurization, the CO_2 shrinking coefficients at 60 and 130 °C are respectively 4.70 and 3.14 10^{-3} MPa^{-1}. At 130 °C, the CO_2 swelling and shrinking coefficients are very close, the difference is about 1.6% in comparison at 60 °C this difference is about 6.2%.

4.2. Effect of the history on thermal coupling and CO_2 sorption tests

Temperature and pressure can be regulated independently with test bench. Consequently, it is possible to evaluate the couplings between thermal and gas intake inflation but also to quantify the impact of a combined thermal and pressure history. A protocol is defined with ten distinct steps (Fig. 9a). Each phase (or step) has as for objective the measurement of different quantities. Table 8 gives all the conditions of temperature, pressure, deviation measurements for the ten steps of the coupling test. Two seals were tested. In the following the steps 1,2,3, … for test 1 and 1′,2′,3′, … for test 2 are named. For both the seals, similar results are obtained in each step. However, due to time constraints, the test on the second seal was shortened and therefore did not undergo step 9'. Thus, after step 8′, step 10′ was conducted from an initial pressure of 2 MPa. This result is then presented (step 10') because it gives information on the coupled behavior. Also, the CO_2 swelling and shrinking coefficients and the thermal expansion coefficient are calculated. Each step is defined below by the temperature and CO_2 pressure applied; where the corresponding properties (thermal expansion coefficient or CO_2 swelling/shrinking coefficient) has been determined:

- Step 1 & 1':
  Conditions: temperature 20–60 °C, pressure 0 MPa,
  Property: coefficient of thermal expansion at 60 °C under air (Table 8).

Fig. 9b shows the measurements of the two O-ring deviations in step 1, i.e. the change from room temperature to 60 °C. Temperature stabilization takes about 3 h. The two measurements devH14 and devH23 almost overlap and have a value of 0.56 and 0.62% respectively for a ΔT of 38.29 °C (Table 8). In test 2 (step 1'), the devH23 measurement has a

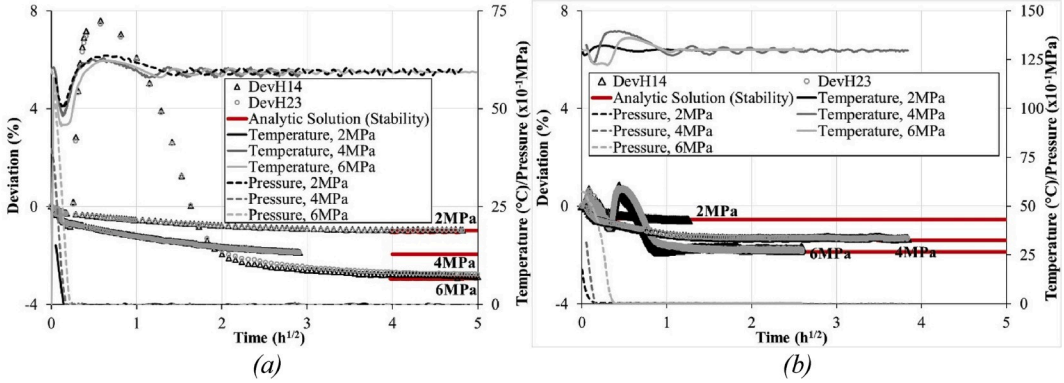

Fig. 7. Evolution of deviation during desorption of 2, 4 and 6 MPa of CO_2 at (a) 60 °C - (b) 130 °C.

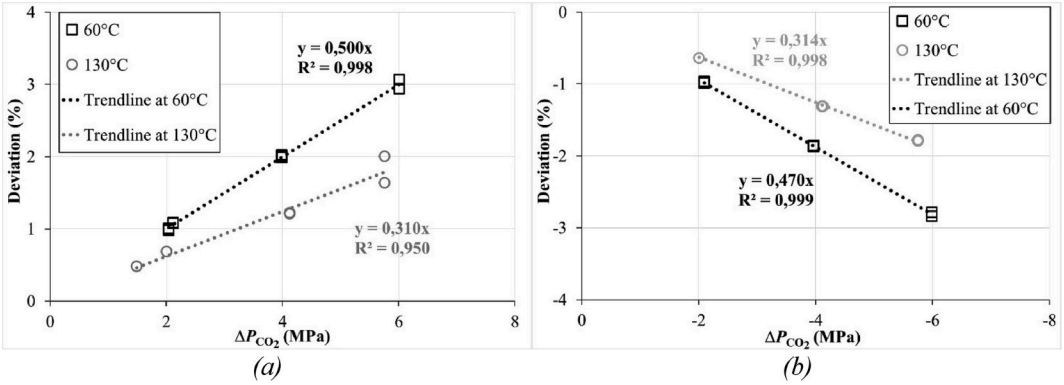

Fig. 8. Deviation as a function of ΔP_{CO2} (a) Determination of the CO_2 swelling coefficient at 60 and 130 °C - (b) Determination of the CO_2 shrinking coefficient at 60 and 130 °C.

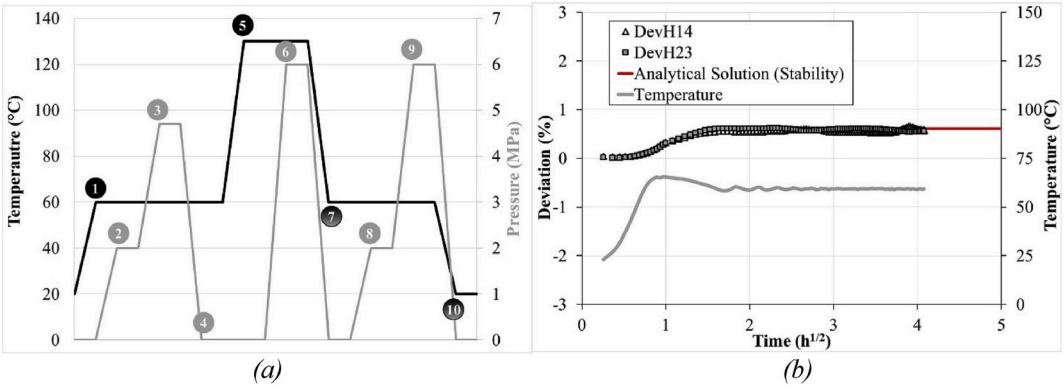

Fig. 9. (a) Test protocol - (b) Step 1: Thermal expansion measurements from 20 to 60 °C under air.

value of 0.75% for a ΔT of 42.36 °C. These values confirm the previous measurement and give an average thermal expansion coefficient equal to 161 10^{-6} °C^{-1}. Both specimens are similar to previous.

- Step 2 & 2':
  Conditions: temperature 60 °C, pressure 0–2 MPa,
  Property: swelling coefficient under 2 MPa of CO_2 pressure at 60 °C (Table 8).

Fig. 10a plots the results of step 2 for test 1. The seal is subjected to a constant temperature of 60 °C and a CO_2 pressure that slowly evolves from 0 to 2 MPa. The stabilization time at CO_2 absorption is about 9 h. The deviations devH14 and devH23 are 0.86 and 0.89% respectively for a ΔP_{CO2} of 2.13 MPa. This gives a CO_2 swelling coefficient between 4.04 and 4.19 10^{-3} MPa^{-1}. These values are lower than those measured previously and given in the previous paragraph. For test 2, the devH23 measurement has a value of 0.96% for a ΔP_{CO2} of 2.02 MPa which gives a CO_2 swelling coefficient of 4.77 10^{-3} MPa^{-1}. The latter value is closer to the coefficients previously measured during CO_2 sorption (Table 5) and CO_2 desorption (Table 6). The lower measurements of the CO_2 swelling coefficient obtained in test 1 may be due to the fact that the stabilization time is not reached (>16 h) unlike test 2 which lasted about 20 h.

- Step 3 & 3':
  Conditions: temperature 60 °C, pressure 2–4 MPa,
  Property: swelling coefficient under 4 MPa of CO_2 pressure at 60 °C (Table 8).

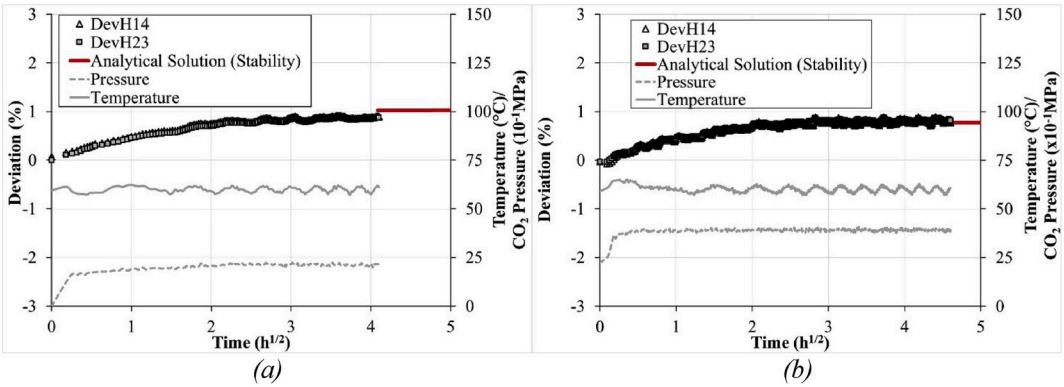

Fig. 10. (a) Step 2: CO_2 sorption measurements from 0 to 2 MPa at 60 °C – (b) Step 3: CO_2 sorption measurements from 2 to 4 MPa at 60 °C.

In step 3, the seal is subjected to an increase in CO_2 pressure from 2.25 MPa to 3.91 MPa or a ΔP_{CO2} of 1.66 MPa for test 1 (Fig. 10b). The stabilization time at 4 MPa (9 h) is lower than that at 2 MPa. This had already been noted earlier. The deviations devH14 and devH23 are 0.80 and 0.82% respectively for a ΔP_{CO2} of 1.66 MPa. The CO_2 swelling coefficients are 4.84 and 4.93 10^{-3} MPa^{-1}. For test 2, the deviations devH14 and devH23 are 1.24 and 1.32% respectively for a ΔP_{CO2} of 2.64 MPa. The CO_2 swelling coefficients are 4.71 and 5.01 10^{-3} MPa^{-1}. These values are in perfect agreement with those obtained previously (Table 5).

For both tests, the cumulative time of steps 2 and 3 is more than 25 h. It can therefore be noted that there is no effect of thermal history on the values of the CO_2 swelling coefficient measurements. The measured deviations are cumulative. Thus, it is possible to bypass step 2 in this protocol.

- Step 4 & 4':
  Conditions: temperature 60 °C, pressure 4 to 0 MPa,
  Property: shrinking coefficient between 4 MPa of CO_2 pressure in air at 60 °C (Table 8).

Fig. 11a shows the deviations during the return of the seal under air pressure at 60 °C (test 1). After a stabilization time of more than 16 h for test 1, the deviations devH14 and devH23 have the values −1.77 and −1.82% respectively for a ΔP_{CO2} of 3.94 MPa. According to equation (18), these two deviation values give as CO_2 shrinking coefficient 4.48 and 4.62 10^{-3} MPa^{-1} respectively. These measurements are very similar to those previously measured (Table 6). There are no measurements for test 2, because the camera lost the markers during the depressurization phase.

- Step 5& 5':
  Conditions: temperature 60–130 °C, pressure 0 MPa,
  Property: thermal expansion coefficient from 60 to 130 °C under air, with the previous history in CO_2 with the history in CO_2 pressure and temperature.

In step 5 (Fig. 11b for test 1), the seal is subjected to a temperature increase from 60 to 130 °C under air. The thermal inertia of the enclosure means that it takes 1 h to reach 130 °C. However, the stabilization time at temperature of the O-ring is less than 4 h. For test 1, the deviations devH14 and devH23 are 1.01 and 1.26% respectively for a ΔT of 69.65 °C. These two values give respectively a coefficient of thermal expansion of 145 and 180 10^{-6} $°C^{-1}$, they are of the same order of magnitude as those measured previously. For test 2, the deviation devH23 is 1.30% for a ΔT of 70.33 °C and gives 184 10^{-6} $°C^{-1}$ as coefficient of thermal expansion. The history of past applied pressure and depressurization on both samples does not appear to affect the thermal expansion property.

- Step 6 & 6':
  Conditions: temperature 130 °C, pressure 0–6 MPa,
  Property: CO_2 swelling coefficient under 6 MPa of CO_2 pressure at 130 °C with the history in CO_2 pressure and temperature (Table 8).

Fig. 12a illustrates the results of the deviation measurements when the seal (test 1) is subjected to a CO_2 pressure of 6 MPa. During this test, the 130 °C temperature could not stabilize as in the other tests. However, it should be noted that the accuracy and sensitivity of the deviation measurements vary significantly, as do thermal fluctuations. The deviations devH14 and devH23 are 1.54 and 1.59% and give respectively as CO_2 swelling coefficients 2.86 and 2.77 10^{-3} MPa^{-1} for a ΔP_{CO2} of 5.55 MPa. For test 2, the deviations devH14 and devH23 are 1.58 and 1.56% and give respectively as CO_2 swelling coefficients 2.81 and 2.78 10^{-3} MPa^{-1} for a ΔP_{CO2} of 5.55 MPa. These values are lower than those previously measured by about 10%. For both tests, temperature control at 130 °C was difficult. Fig. 12a shows the temperature variations that lead to slight variations in CO_2 pressure throughout the test. These disturbed the deviation measurements, which may explain these lower values, whereas previously the measurements were highly reproducible.

- Step 7 & 7':
  Conditions: temperature 130 to 60 °C, pressure 6 to 0 MPa,
  Property: coupling dilatation and desorption of the seal subjected to a CO_2 depressurization of 6 MPa in air and a temperature passing from 130 to 60 °C (Table 8).

Fig. 12b describes the results of the deviation measurements when a thermal ramp of 130 to 60 °C and the return of the seal under air are imposed simultaneously from an initial CO_2 pressure of about 6 MPa for test 1. As already discussed above, the temperature decreases by about ten degrees as the CO_2 pressure decreases. Within this time, the seal retracts and then once it has returned under air it swells to achieve a deviation of about 1.1%. The figure illustrates that it takes almost more than 9 h for the enclosure to stabilize at 60 °C. The thermal velocity being very slow, the temperature of the seal is almost the same as the one measured in the enclosure. Thus, the temperature stabilization time of the seal is of the same order as that of the enclosure. For test 1, the deviations devH14 and devH23 are −3.33 and −3.32% respectively for a ΔP_{CO2} of 6.32 MPa and ΔT of 67.86 °C. For test 2, the deviation devH23 is −2.74% for a ΔP_{CO2} of 5.62 MPa and ΔT of 67.91 °C. Notice that during the transient phase, it is not possible to determine simultaneously the thermal expansion and CO_2 shrinking coefficients without a numerical model that would allow the transition phase to be taken into account. However, it is possible to estimate the deviation at the end of the step in the stabilization phase, by the sum of the values of thermal strain and "pressure strain" calculated respectively with expressions (6) and (15) and using the thermal expansion and CO_2 shrinking coefficients

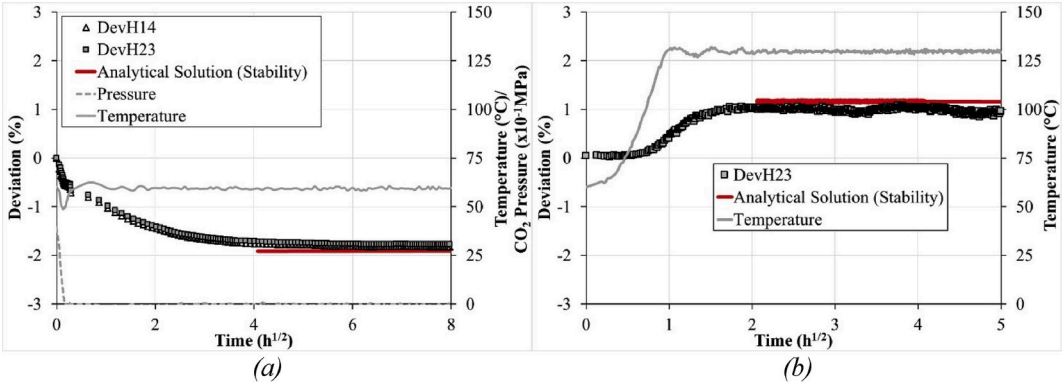

Fig. 11. (a) Step 4:CO_2 desorption measurements from 4 to 0 MPa at 60 °C – (b) Step 5: Thermal expansion measurements from 60 to 130 °C under air.

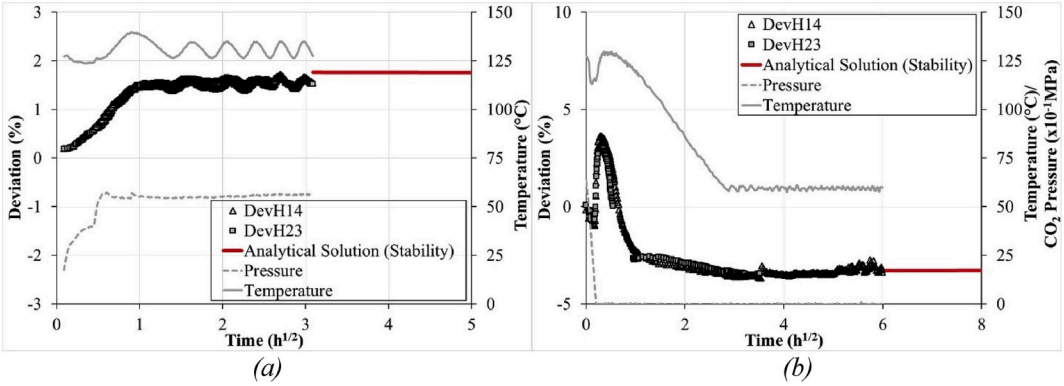

Fig. 12. (a) Step 6: CO_2 sorption measurements from 2 to 6 MPa at 130 °C – (b) Step 7: Thermal expansion measurements and CO_2 desorption measurements during change from 6 to 0 MPa and from 130 to 60 °C.

identified above. A constant thermal expansion coefficient of 170 10^{-6} $°C^{-1}$ and the shrinking coefficient as a function of temperature is chosen from the existing data. Thus the shrinking parameters a_{CO_2} and b_{CO_2} (equation (8)) are $-2.23\ 10^{-5}$ and $6.04\ 10^{-3}$ respectively. For test 1, the deviation obtained is equal to −3.27%. Fig. 12b displays that this value (analytical solution) is very close to the experimental response. At this stage, it can be said that there is no effect of gas and thermal histories on measurements and the law is additive without coupling the two phenomena.

- Step 8 & 8':
  Conditions: temperature 60 °C, pressure 0–2 MPa,
  Property: CO_2 swelling coefficient under 2 MPa of CO_2 pressure at 60 °C, after desorption and complex history of temperature and pressure (Table 8).
- Step 9 & 9':
  Conditions: temperature 60 °C, pressure 0–6 MPa,
  Property: CO_2 swelling coefficient under 6 MPa of CO_2 pressure at 60 °C, after a complex history of temperature and pressure (Table 8).

Steps 8 (Fig. 13a, test 1) and 9 (Fig. 13b, test 1) consist at 60 °C in imposing respectively a first ramp going from air to a CO_2 pressure of about 2 MPa, then after a stabilization time a second one going up to about 6 MPa. The conditions imposed in step 8 on the O-ring are the same as those in step 2. The only difference is that the seal undergone a complex thermal and CO_2 history. Fig. 13a shows a deviation curve almost identical to those in Fig. 12a (step 2). The stabilization time at CO_2 absorption is about 9 h, same as in step 2. The two measurements devH14 and devH23 almost overlap and have a value of 1.03 and 1.07% respectively for a ΔP_{CO2} of 2.11 MPa (Table 8). During the transition from about 2 MPa to about 6 MPa, Fig. 13b indicates that the values of the deviations almost doubled for ΔP_{CO2} of 3.94 MPa compared to step 8 (ΔP_{CO2} of 2.11 MPa). The deviations devH14 and devH23 are 1.94 and 2.03% respectively. The values of the deviations obtained in steps 8 and 9 lead to CO_2 swelling coefficient values of the same order. Thus for steps 8 and 9, the average values are 4.96 (4.85–5.08) 10^{-3} MPa^{-1} and 5.04 (4.93–5.15) 10^{-3} MPa^{-1}. The values measured in test 2 confirm on the one hand the measurements performed in test 1 (and consequently the reproducibility of these measurements), and on the other hand that the particular effect of the thermal and CO_2 environment stories is of the second order.

- Step 10 & 10':
  Conditions: temperature 60 to 20 °C, pressure 6 to 0 MPa (test 1) and pressure 2 to 0 MPa (test 2),
  Property: coupling dilatation and desorption of the seal subjected to a CO_2 depression of 6 MPa (and 2 MPa) in air and a temperature passing from 60 to 20 °C.
  Reminder: seal 1 (test 1) has undergone the test protocol with the 10 steps, seal 2 (test 2) has undergone the test protocol without step 9′ and therefore the initial pressure of step 10′ is 2 MPa instead of 6.

The last step (test 1) consists in bringing the seal back to room temperature under air when it was subjected simultaneously to a temperature of 60 °C and a CO_2 pressure of about 6 MPa. A second test was performed with an initial pressure of CO_2 at 2 MPa (step 10'). The beginning of the two ramps, thermal and CO_2 pressure are imposed simultaneously. Fig. 14a shows the responses of the deviations in the last step of this coupling test. The temperature decreases sharply by about ten degrees from the beginning of the test as the CO_2 pressure decreases.

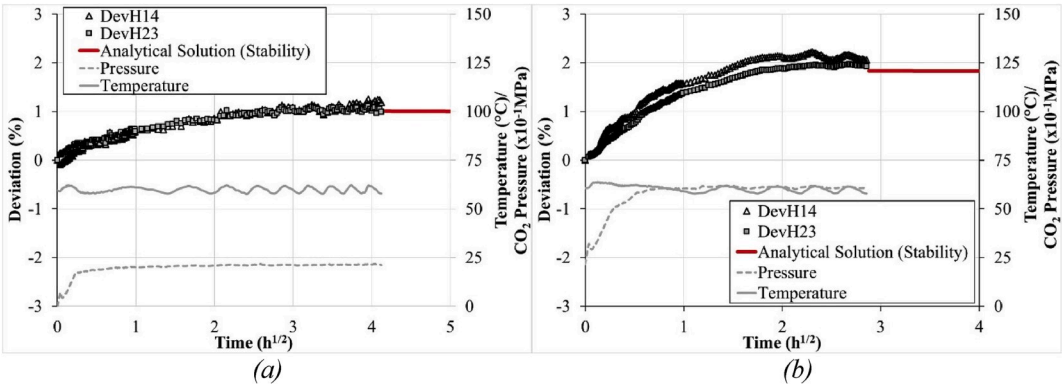

Fig. 13. (a) Step 8: CO_2 sorption measurements from 0 to 2 MPa at 60 °C – (b) Step 9: CO_2 sorption measurements from 2 to 6 MPa at 60 °C.

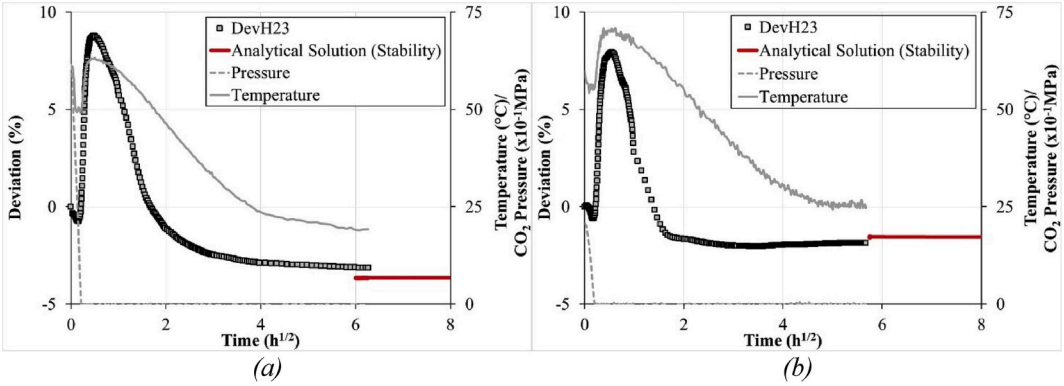

Fig. 14. Step 10: (a) Test 1: Thermal expansion measurements and CO_2 desorption measurements during change from 6 to 0 MPa and from 60 to 20 °C – (b) Test 2: Thermal expansion measurements and CO_2 desorption measurements during change from 2 to 0 MPa and from 60 to 20 °C.

In this phase, the O-ring retracts by just 1% before inflating by about 8–9% after the return to the air (zero CO_2 pressure). Then it slowly deflates due to CO_2 desorption and temperature decrease. The stabilization time is more than 16 h. Finally, the deviations devH14 and devH23 are −3.13 and 4% respectively for a ΔP_{CO2} of 6.13 MPa and ΔT of 41.78 °C. The two dilations combine during this phase.

As in step 7, it is possible to calculate for the two tests in step 10 the total strain in the stabilized phase by summing equations (6) and (15). Thus, the strain for test 1 and test 2 is respectively −3.66% and −1.57%. Fig. 14a demonstrates that at the end of the test, the return to room temperature had not yet been achieved. Besides, it is possible that the CO_2 desorption was not complete, or the seal may have residual deformation because of dammage. The slope of the deformation as a function of time between 16 and 36 h is decreasing. The analytical solution gives a higher final deformation. On the other hand, Fig. 14b shows that at the end of the test, the return to room temperature is achieved. The strain is almost stabilized and the final value is close to the analytical solution. In test 2, the initial pressure is 2 MPa whereas in the test 1 it was 6 MPa.

To go to further analysis, in Fig. 15a, the responses of a CO_2 depressurization from 6 MPa to 0 MPa at constant temperature (60 °C) and a CO_2 depressurization from 6 MPa to 0 MPa coupled with a temperature ramp from 60 to 20 °C are superimposed. In Fig. 15b, the responses of a CO_2 depressurization from 2 MPa to 0 MPa at constant temperature (60 °C) and a CO_2 depressurization from 2 MPa to 0 MPa coupled with a temperature ramp from 60 to 20 °C are plotted. In both figures, the red lines represent the responses from the analytical solutions in the isothermal depressurization test and in the coupled test (depressurization and temperature decrease). Fig. 15a illustrates that the responses are almost identical in the transient phase until 9 h. However, if in the constant temperature test the deviation is stabilized after 25 h, the same is not true for the coupled test. This is due to the thermal inertia of the autoclave. The maximum deviations measured in the transient phase for the isothermal depressurization test and the coupled test are 7.44 and 8.73%, respectively. The maximum swelling of the O-ring is approximately 24 and 28.5% respectively. Finally, in both tests, the temperature at the time of depressurization drops rapidly between 10 (isothermal depressurization test) and 15 °C (coupled test) and then rises to a maximum value of 62–63 °C.

On the other hand, Fig. 15b shows quite different responses. Thus, while at constant temperature, depressurization does not cause the seal to swell at an initial pressure of 2 MPa, when coupled with temperature, a swelling appears almost of the same order of magnitude as at constant temperature (60 °C). The maximum deviation measured is 8% or a swelling of about 26%. As before, in both tests the temperature at the time of depressurization drops rapidly between 5 (isothermal depressurization test) and 10 °C (coupled test), but there is a larger difference in the maximum value reached. Thus, in the constant temperature depressurization test the value is close to 63 °C, in the coupled test it reaches 71 °C.

Finally, when an O-ring is subjected to a pressure of 6 MPa and is subjected to isothermal depressurization or coupled with a temperature decrease, this leads to a swelling of the O-ring in the same orders of magnitude (24–28%). On the other hand, at a pressure of 2 MPa, in the isothermal depressurization test the seal does not swell, in the coupled test the swelling (26%) in the transient phase is from the level of the tests to 6 MPa. Thus, this shows that in addition to pressure, CO_2 thermo-depressurization conditions are very important and not negligible in the lifetime of an O-ring seal.

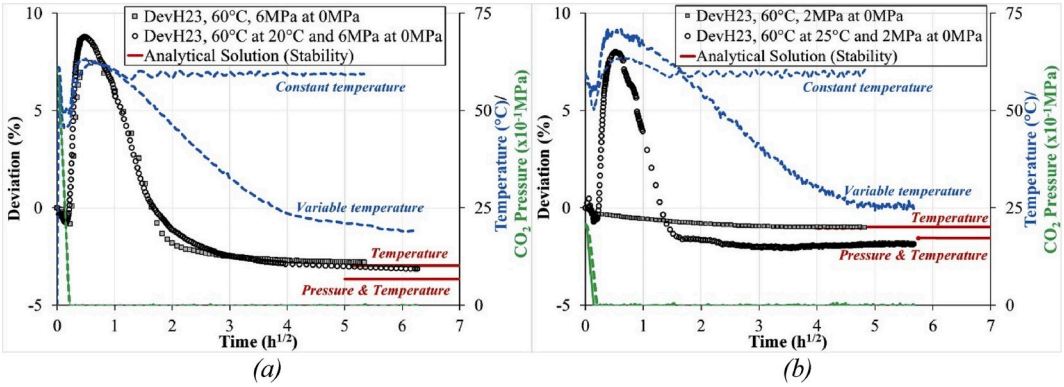

Fig. 15. Thermal expansion measurements and CO_2 desorption measurements (a) for tests during change from 6 to 0 MPa and from 60 to 20 °C and from to 6 to 0 MPa at 60 °C – (b) for tests during change from 2 to 0 MPa and from 60 to 20 °C and from 2 to 0 MPa at 60 °C.

5. Discussions

A general overview of the O-ring life under thermo-diffuso constrains is discussed, based on: *i. ageing under CO_2, ii. Deviation coefficients of swelling and shrinking versus imposed CO_2 pressure, iii. Thermal coefficient of shrinking versus imposed coupled thermo-CO_2 pressure, and iv. From deviation coefficient to volume variation, comparison with literature data.*

i. Ageing under CO_2

Table 8 shows that in step 4, the value of CO_2 shrinking coefficient is between 4.49 and 4.62 10^{-3} MPa^{-1}. These values are similar to the average value of 4.70 10^{-3} MPa^{-1}. Although this value is slightly lower than that of CO_2 sorption, it does not seem to be due to ageing under CO_2. The deflation measurements made in steps 5, 6, 8 and 9 lead to coefficients of thermal expansion and CO_2 swelling (different conditions) quite similar to those obtained previously. Finally, although only two temperatures have been achieved, it can be seen that the CO_2 swelling and shrinking coefficients increase as the temperature decreases.

ii. Deviation coefficients of swelling and shrinking versus imposed CO_2 pressure

Fig. 16 are equivalent to Fig. 11 supplemented with data from the coupled test. The values obtained during the two coupled tests are represented by a hatched triangle (test 1) and a hatched diamond (test 2). The observed trends show that for a given temperature, the deviations increase proportionally with the imposed CO_2 pressure.

Thus, Fig. 16a shows that after CO_2 sorption, the CO_2 swelling coefficients at 60 and 130 °C are respectively 4.95 and 2.94 10^{-3} MPa^{-1}. Fig. 16b describes that after the complete desorption of CO_2, the CO_2 shrinking coefficients at 60 and 130 °C are respectively 4.67 and 3.14 10^{-3} MPa^{-1}. Overall, the CO_2 swelling and shrinking coefficients are almost identical to those identified in the two previous paragraphs to within 1%. Only the swelling coefficient at 130 °C decreased from 3.10 to 2.94 10^{-3} MPa^{-1}. Since not all conditions (pressure, temperature) have the same number of measuring points, these results can therefore be considered to fall within the range of measurement errors.

iii. Thermal coefficient of shrinking versus imposed coupled thermo-CO_2 pressure

Steps 7,7′, 10 and 10’ of the test coupled on the O-ring consisted in imposing a ramp from an initial CO_2 pressure of about 6 MPa until return to the air coupled respectively to a temperature ramp of 130 to 60 °C and 60 °C at room temperature. In first approximation the value of the deviation obtained in these two steps is given by the sum of equations (6) and (7), i.e.:

$$dev = \varepsilon_{th} + \varepsilon_{pressure\_CO_2} = \alpha_{th}\left(T_{final} - T_{initial}\right) + \alpha_{shrinking\_CO_2}\left(P_{final} - P_{initial}\right). \quad (22)$$

As explain before, it is not possible at this juncture to directly identify the thermal expansion coefficient (α_{th}) and the CO_2 shrinking coefficient ($\alpha_{shrinking\_CO_2}$). However, it is possible to compare simulations obtained with simple combinaison of volumic strain and experimental deviation from the actual conditions in temperature and pressure and using the previously identified coefficients of thermal expansion and CO_2 shrinking.

However, for step 10 where the pressure and temperature decrease respectively from 6.13 to 0 MPa and from 61 to 19.22 °C, it is possible to estimate the deviation. Thus, taking as CO_2 shrinking coefficient 4.66 10^{-3} MPa^{-1} and as thermal expansion coefficient 163 10^{-6} $°C^{-1}$, a deviation value is obtained with −3.54%. Despite the difference between the deviation measurements obtained (3.13 and 4.70%), the theoretical value is within this range. The observation confirms that the strains (deviations) resulting from thermal and CO_2 desorption are cumulative.

iv. From deviation coefficient to volume variation, comparison with literature data

Fig. 17 illustrates the comparision between the HNBR results of this study with the HNBR1 studied by Schrittesser et al. [13] and the NBR and EPDM studied by Dubois et al. [14]. Fig. 17a shows the volume variation due to CO_2 sorption after stabilization as a function of temperature at different CO_2 pressures. Fig. 17b shows the volume variation due to CO_2 sorption after stabilization as a function of CO_2 pressure for different temperatures. As a reminder, the change in volume (swelling) due to CO_2 pressure is calculated from the measurement of the deviation (equation (21)).

Although HNBR1 [13] has a higher hardness than HNBR in this study, it appears that the measurements obtained here are in perfect adequacy with those obtained by Schrittesser et al. [13] for different conditions in pressure and temperature.

6. Conclusions

In this work a new technique is presented. It allows the measurement of the swelling or shrinking of an elastomeric O-ring seal during CO_2 sorption and desorption respectively. Besides, in order to be as close as possible to real conditions of use (process), the tests are carried out on an HNBR O-ring rather than on laboratory specimens (plate, cylinder). This non-contact extensometry method, with markers placed on the O-ring, measures local strain. The numerical simulation confirmed that with such measurement, the identification of the swelling (or shrinking) coefficient is possible. Thermal expansion tests explorated at 60 and 130 °C

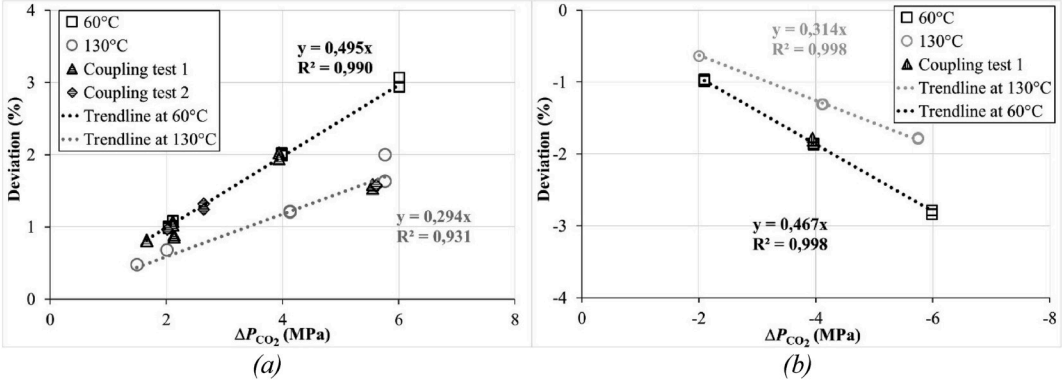

Fig. 16. Deviation as a function of ΔP_{CO_2} (a) Determination of the CO_2 swelling coefficient at 60 and 130 °C - (b) Determination of the CO_2 shrinking coefficient at 60 and 130 °C.

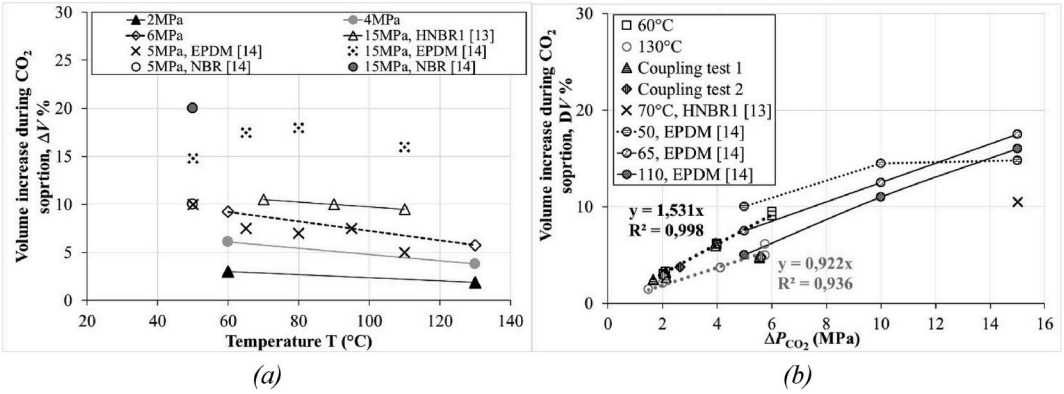

Fig. 17. (a) Volume change as a function of temperature after stabilization of CO_2 absorption - (b) Volume change as a function of pressure after stabilization of CO_2 absorption.

and performed on O-rings and the obtained deviation measurements confirmed the numerical results. The comparison of the thermal expansion coefficients thus obtained with the values measured by a standard thermal expansion test and a non-standard test (DMA compression) validated the measurement method. However, only the values of horizontal deviations can be used.

Therefore, tests under different temperatures (60 and 130 °C) and different CO_2 sorption pressures (2, 4 and 6 MPa) and desorption were performed. All these tests highlight that, in this range of pressure and temperature, the exposure time under pressure and temperature had almost no influence on the swelling coefficient. This is almost constant as a function of pressure. On the other hand, this coefficient is very dependent of the temperature, since at 130 °C (2.94 10^{-3} MPa^{-1}) it is about 60% of that at 60 °C (4.95 10^{-3} MPa^{-1}).

Coupled tests, in the temperature range 60–130 °C and in the CO_2 pressure range up to 6 MPa, showed that the HNBR seal was not impacted by the cycle and stabilization conditions (temperature and CO_2 pressure) that could cause the material to ageing. The values of thermal expansion coefficients, swelling and shrinking coefficients under CO_2 are almost the same as during isothermal tests at different pressures. In addition, the results of these tests showed that the law is additive without coupling the two phenomena (thermal, pressure). Finally, it has been shown that it is not only the pressure level that can cause significant swelling during depressurization. Thus, even under only 2 MPa pressure the seal can have a significant swelling if the depressurization is coupled with a temperature drop. The CO_2 thermo-depressurization conditions are therefore very important and not negligible in the lifetime of an O-ring seal.

Moreover, this deviation measurement allows, in the context of an isotropy hypothesis, to determine the swelling and shrinking of the seal induced by the sorption and desorption of CO_2, respectively. By comparing the results with the literature for HNBR (by Schrittesser et al. [13]) and other elastomers, although the conditions in temperature and CO_2 pressure are not the same, show that the measurements obtained by this method are quite in the same order as the swellings already observed. The compilative data validate our method.

Subsequently, a comparison with a model should permit to study the transient phase and to evaluate the diffusion time.

Declaration of competing interest

The authors declare that they have no known competing financial interests or personal relationships that could have appeared to influence the work reported in this paper.

CRediT authorship contribution statement

E. Lainé: Project administration, Writing - original draft, Visualization, Methodology. **J.C. Grandidier:** Project administration, Supervision, Visualization. **G. Benoit:** Methodology. **B. Omnès:** Project administration, Writing - review & editing, Supervision. **S.A.E. Boyer:** Supervision, Writing - review & editing, Methodology.

Acknowledgements

We thank Schlumberger Company and Schlumberger Geoservices Company for their Sponsoring in the Citeph project OGSANE (CITEPH-36-2012) and led by the Cetim. In this project Cetim and Pprime establish a R&D collaboration to study the seal behaviour with gas. The aim of this private project was the study of the improvement of performance of rubber seal with nanofiller in rubber in Oil&Gas conditions.

This work was supported by the CPER FEDER project of Région Nouvelle Aquitaine.

Appendix

Table 5
HNBR - Deviations and CO_2 swelling coefficients for the different CO_2 pressurization tests (2 temperatures and 3 CO_2 pressures)

Test	Temperature	ΔP	DevH14	DevH23	CO_2 swelling coefficients		
					/DevH14	/DevH23	Average
	(°C)	(MPa)	(%)	(%)	(10^{-3} MPa^{-1})		
1	59.93	2.116	1.081	1.075	5.109	5.080	5.095
2	60.22	2.040	1.001	0.981	4.907	4.809	4.858
3	60.34	3.988	1.892	1.876	4.970	4.990	4.980

(*continued on next page*)

Table 5 (*continued*)

Test	Temperature	ΔP	DevH14	DevH23	CO_2 swelling coefficients		
					/DevH14	/DevH23	Average
	(°C)	(MPa)	(%)	(%)	(10^{-3} MPa^{-1})		
4	59.80	3.993	2.003	2.019	5.016	5.056	5.035
5	60.32	6.009	3.059	2.938	5.091	4.889	4.990
6	130.05	1.487	/*	0.480	/*	3.228	3.228
7	130.00	2.009	/*	0.683	/*	3.400	3.400
8	130.14	4.125	1.209	1.223	2.931	2.965	2.948
9	130.06	5.756	2.001	1.636	3.476	2.842	3.159

*Value not retained due to the loss of the image.

Table 6
HNBR - Deviations and CO_2 shrinking coefficients for the different CO_2 desorption tests (2 temperatures and 3 CO_2 pressures)

Test	Temperature	ΔP	DevH14	DevH23	CO_2 shrinking coefficient		
					/DevH14	/DevH23	Average
	(°C)	(MPa)	(%)	(%)	(10^{-3} MPa^{-1})		
1	59.95	−2.093	−0.966	−0.991	4.614	4.734	4.674
2	59.96	−3.966	−1.858	−1.875	4.686	4.727	4.707
3	59.94	−5.993	−2.840	−2.785	4.722	4.630	4.676
4	129.81	−1.782	/*	−0.568	/*	3.190	3.187
5	129.36	−4.105	−1.311	−1.313	3.192	3.197	3.195
6	130.03	−5.722	−1.797	−1.779	3.140	3.109	3.125

*Value not retained.

Table 7
HNBR - Deviations (swelling) and minimal temperature during the depressurization phase for the different CO_2 desorption tests (2 temperatures and 3 CO_2 pressures)

Initial Conditions		Min Temperature (*T*)			Max swelling (*Sw*)		
Temperature (°C)	Pressure (MPa)	Time (s)	Min. T (°C)	Pressure (MPa)	Time (s)	/DevH14 (%)	/DevH23 (%)
58.78	2.093	60.33	50.43	0.241	No swelling		
60.15	3.967	59.73	48.27	0.739			
57.94	5.993	49.91	44.60	3.074	1175	7.78	7.60
129.78	1.782	92.91	127.22	1.034	No swelling		
134.28	4.132	68.4	123.23	0.369			
129.74	5.741	71.14	122.77	4.802	855	0.696	0.702

Table 8
Temperature, pressure and deviations conditions and coefficient values measurements for each step of the coupling test.

Step	Temperature (°C)		Pressure (MPa)		Deviation (%)		CO_2 swelling coefficient (MPa^{-1})/
	Initial	Final	Initial	Final	DevH14	DevH23	*Thermal expansion coefficient* ($°C^{-1}$)
1	21.11	59.40	0		0.560	0.615	*145 – 160 10^{-6}*
1′	17.00	59.36	0		/	0.749	*- – 177 10^{-6}*
2	59.38		0	2.13	0.860	0.892	4.04–4.19 10^{-3}
2′	59.80		0	2.02	/	0.963	- – 4.77 10^{-3}
3	59.84		2.25	3.91	0.804	0.818	4.84–4.93 10^{-3}
3′	59.64		2.01	4.65	1.240	1.320	4.71–5.01 10^{-3}
4	60.02		3.94	0	−1.770	−1.820	4.49–4.62 10^{-3}
4′	60.12		4.87	0	/	/	–
5	60.08	129.73	0		1.006	1.258	*145 – 180 10^{-6}*
5′	59.38	129.71	0		/	1.295	*- – 184 10^{-6}*
6	130.67		0	5.55	1.589	1.536	2.77–2.86 10^{-3}
6′	132.32		0	5.61	1.579	1.558	2.78–2.81 10^{-3}
7	127.76	59.90	6.32	0	−3.331	−3.320	–
7′	127.27	59.36	5.62	0	/	−2.741	–
8	59.86		0	2.11	1.027	1.074	4.85–5.08 10^{-3}
8′	/		/	/	/	/	–
9	59.75		2.15	6.09	1.941	2.029	4.93–5.15 10^{-3}
9′	/		/	/	/	/	–
10	61.00	19.22	6.13	0	/	−3.134*	–
10′	59.70	24.57	2.08	0	/	−1.870	–

*Value at the end of the test (unstabilized state).

References

[1] B. Alcock, T.A. Peters, R.H. Gaarder, J.K. Jørgensen, The effect of hydrocarbon ageing on the mechanical properties, apparent crosslink density and CO_2 diffusion of a hydrogenated nitrile butadiene rubber (HNBR), Polym. Test. 47 (2015) 22–29.

[2] T. Grelle, D. Wolff, M. Jaunich, Temperature-dependent leak tightness of elastomer seals after partial and rapid release of compression, Polym. Test. 48 (2015) 44–49.

[3] S.Z. Qamar, M. Akhtar, T. Pervez, M.S.M. Al-Kharusi, Mechanical and structural behavior of a swelling elastomer under compressive loading, Mater. Des. 45 (2013) 487–496.

[4] B. Flaconnèche, J. Martin, M.H. Klopffer, Transport properties of gases in polymers: experimental methods, oil & gas science and technology – rev, IFPEN 56 (3) (2001) 245–259.

[5] Z. Filus, T. Ajtai, Z.L. Horvath, Z. Bozoki, G. Pap, T. Nagy, T. Katona, G. Szabo, A novel apparatus based on a photoacoustic gas detection system for measuring permeation parameters of polymer samples, Polym. Test. 26 (5) (2007) 606–613.

[6] B.J. Briscoe, S. Zakaria, Interaction of CO_2 gas with silicone elastomer at high ambient pressures, J. Polym. Sci., Part B: Polym. Phys. 29 (1991) 989–999.

[7] B.J. Briscoe, T. Savvas, C.T. Kelly, Explosive decompression failure of rubber: a review of the origins of pneumatic stress-induced rupture in elastomers, Rubber Chem. Technol. 67 (3) (1994) 384–416.

[8] Z. Major, R.W. Lang, Characterization of the fracture behavior of NBR and FKM grade elastomers for oilfield applications, Eng. Fail. Anal. 17 (3) (2010) 701–711.

[9] O.M. Davies, J.C. Arnold, S. Sulley, The mechanical properties of elastomers in high-pressure CO_2, J. Mater. Sci. 34 (2) (1999) 417–422.

[10] B.J. Briscoe, C.T. Kelly, The effect of structure on gas solubility and gas induced dilation in a series of poly(urethane) elastomers, Polymer 37 (15) (1996) 3405–3410.

[11] B. Bonavoglia, G. Storti, M. Morbidelli, A. Rajendran, M. Mazzotti, Sorption and swelling of semicrystalline polymers in supercritical CO_2, J. Polym. Sci., Part B: Polym. Phys. 44 (11) (2006) 1531–1546.

[12] S. Shenoy, D. Woerdeman, R. Sebra, A. Garach-Domech, K.J. Wynne, Quantifying polymer swelling employing a linear variable differential transformer: CO_2 effects on SBS triblock copolymer, Macromol. Rapid Commun. 23 (18) (2002) 1130–1133.

[13] B. Schrittesser, G. Pinter, Th Schwarz, Z. Kadar, T. Nagy, Rapid gas decompression performance of elastomers – a study of influencing testing parameters, Procedia Struct. Integr. 2 (2016) 1746–1754.

[14] J. Dubois, E. Grau, T. Tassaing, M. Dumon, On the CO_2 sorption and swelling of elastomers by supercritical CO_2 as studied by in situ high pressure FTIR microscopy, J. Supercrit. Fluids 131 (2018) 150–156.

[15] A. Rajendran, A. Bonavoglia, B. Forrer, N. Storti, G. Mazzotti, M. Morbidelli, Simultaneous measurement of swelling and sorption in a supercritical CO_2-poly (methyl methacrylate) system, Ind. Eng. Chem. Res. 44 (8) (2005) 2549–2560.

[16] F. Daou, C.R. de Miranda, J.L. de Oliveira, B. Engelke, C. Borman, S. Le Roy-Delage, Swelling of Elastomers in CO_2 Environment: Testing Methodology and Experimental Data, SPE Latin America and Caribbean Petroleum Engineering Conference 21–23 May, Maracaibo, Venezuela, 2014.

[17] K.J. Thurecht, D.J.T. Hill, A.K. Whittaker, Equilibrium swelling measurements of network and semicrystalline polymers in supercritical carbon dioxide using highpressure NMR, Macromolecules 38 (9) (2005) 3731–3737.

[18] S.K. Goel, E.J. Beckman, Modelling the swelling of crosslinked elastomers by supercritical fluids, Polymer 33 (23) (1992) 5032–5039.

[19] L.M. Robeson, Q. Liu, B.D. Freeman, D.R. Paul, Comparison of transport properties of rubbery and glassy polymers and the relevance to the upper bound relationship, J. Membr. Sci. 476 (2015) 421–431.

[20] S. Hilic, S.A.E. Boyer, A.A.H. Padua, J.P.E. Grolier, Simultaneous measurement of the solubility of nitrogen and carbon dioxide in polystyrene and of the associated polymer swelling, J. Polym. Sci., Part B: Polym. Phys. 39 (17) (2001) 2063–2070.

[21] R.M.H. Felder, in: R.A. Fava (Ed.), Permeation, Diffusion, and Sorption of Gases and Vapors, Methods Exp. Physics, Part C: Polymer Physics, Academic Press, New York, 1980.

[22] Y. Kamiya, K. Mizoguchi, K. Terada, Y. Fujiwara, J.-S. Wang, CO_2 sorption and dilation of poly(methyl methacrylate), Macromolecules 31 (2) (1998) 472–478.

[23] N.H. Brantley, S.G. Kazarian, C.A. Eckert, In situ FTIR measurement of carbon dioxide sorption into poly(ethylene terephthalate) at elevated pressures, J. Appl. Polym. Sci. 77 (4) (2000) 764–775.

[24] R.G. Wissinger, M.E. Paulaitis, Swelling and sorption in polymer-CO_2 mixtures at elevated pressures, J. Polym. Sci., Part B: Polym. Phys. 25 (12) (1987) 2497–2510.

[25] J.R. Royer, J.M. DeSimone, S.A. Khan, Carbon dioxide-induced swelling of poly (dimethylsiloxane), Macromolecules 32 (26) (1999) 8965–8973.

[26] D.H. Ender, Elastomeric seals, Chemtech 16 (1) (1986) 52–57.

[27] S.A.E. Boyer, M.H. Klopffer, J. Martin, J.P.E. Grolier, Supercritical gas-polymer interactions with applications in the petroleum industry. Determination of thermophysical properties, J. Appl. Polym. Sci. 103 (3) (2007) 1706–1722.

[28] J.-C. Grandidier, C. Baudet, S.A.E. Boyer, M.-H. Klopffer, L. Cangémi, Diffusion kinetics and thermo-diffuso mechanical behavior of polyvinylidene fluoride/ carbon dioxide system during explosive decompression: a first numerical approach with an experimental confrontation, Oil & Gas Science and Technology – Rev, IFPEN 70 (2) (2015) 251–266.

[29] E. Lainé, J.C. Grandidier, G. Benoit, B. Omnès, F. Destaing, Effects of sorption and desorption of CO_2 on the thermomechanical experimental behavior of HNBR and FKM O-rings - influence of nanofiller-reinforced rubber, Polym. Test. 75 (2019) 298–311.

[30] S. Castagnet, J.-C. Grandidier, M. Comyn, G. Benoît, Effect of long-term hydrogen exposure on the mechanical properties of polymers used for pipes and tested in pressurized hydrogen, Int. J. Pres. Ves. Pip. 89 (2012) 203–209.

[31] S.A.E. Boyer, M. Gerland, S. Castagnet, Gas environment effect on cavitation damage in stretched PolyVinylidene Fluoride, Polym. Eng. Sci. 54 (2014) 2139–2146.

[32] Abaqus/CAE User's Guide, Ver. 6.13, vol. 3, Dassault Systèmes Simulia Corp., Providence, RI, USA, 2013.

[33] L.R.G. Treloar, The Physics of Rubber Elasticity, Oxford University Press, 1975.

[34] O.H. Yeoh, Developments in Finite Element Analysis, Engineering with Rubber, Carl Hanser Verlag GmbH & Co. KG, 2012, pp. 345–364.

[35] Norme ISO 11-359-2, Plastics - Thermomechanical Analysis (TMA) - Part 2: Determination of Coefficient of Linear Thermal Expansion and Glass Transition Temperature, 1999.

[36] Z. Sun, G. Benoit, C. Moriconi, F. Hamon, D. Halm, F. Hamon, G. Hénaff, Fatigue crack propagation under gaseous hydrogen in a precipitation-hardened martensitic stainless steel, Int. J. Hydrogen Energy 36 (14) (2011) 8641–8644.

[37] S. Castagnet, J.C. Grandidier, M. Comyn, G. Benoit, Mechanical testing of polymers into pressurized hydrogen: tension, creep and ductile fracture, Exp. Mech. 52 (3) (2012) 229–239.

[38] G. Benoit, S.A.E. Boyer, S. Castagnet, G. Henaff, E. Lainé, F. Mauget, Mechanical testing in pressurized hydrogen and carbon dioxide, in: The 10th BSSM International Conference on Advances in Experimental Mechanics, Edinbourg, Ecosse, 2015, 1-3 Septembre.

[39] Evaluating elastomeric materials in carbon dioxide decompression environments, Nace Standard TM0192–98 (1998).

[40] Qualification of non-metallic sealing materials and manufacturers, Norsok Stand. M-710 Rev. 3 (2014) sept.